Supporting Information of

Mechanistic Investigations of Thermal Decomposition of Perfluoroalkyl Ether Carboxylic Acids and Short-chain Perfluoroalkyl Carboxylic Acids

Ali Alinezhad[a,+], Heng Shao[b,+], Katerina Litvanova[c], Runze Sun[a], Alena Kubatova[c], Wen Zhang[d], Yang Li[b,*], Feng Xiao[a,*]

[a] Department of Civil and Environmental Engineering, The University of Missouri, Columbia, Missouri 65211, USA

[b] Key Laboratory of Water and Sediment Sciences of Ministry of Education, State Key Laboratory of Water Environment Simulation, School of Environment, Beijing Normal University, Beijing 100875, People's Republic of China

[c] Department of Chemistry, The University of North Dakota, Grand Forks, North Dakota 58202, USA

[d] John A. Reif, Jr. Department of Civil and Environmental Engineering, New Jersey Institute of Technology, Newark, NJ 07102, USA

[+]: The authors contributed equally to this work and share first authorship.

[*]Corresponding authors

Number of pages: 22

Number of tables: 8

Number of figures: 10

Contents

UPLC–QToF-MS/MS method.

PFAS and polar thermal decomposition products were analyzed on a Waters Acquity UPLC coupled with a Waters QToF-MS/MS (Synapt G2-S, Waters Corporation, Milford, MA, USA). Chromatography was performed using a Waters Acquity UPLC BEH Shield RP18 column (100 × 2.1 mm; 130 Å; 1.7 μm) with a Waters Acquity UPLC BEH Shield RP18 VanGuard pre-column (5 × 2.1 mm; 130 Å; 1.7 μm). The mobile phase consisted of eluent A (2 mM ammonium formate in OptimaTM water; LC/MS grade) and eluent B (2 mM ammonium formate in OptimaTM methanol; LC/MS grade). The elution started at 20% B for 0.5 min and then was linearly increased to 85% B in 5 min, further increased to 98% B in 0.1 min and kept isocratic for 1.5 min. At 7.1 min, the A/B ratio changed back to the initial value of 80/20 over 0.1 min to re-equilibrate the column for another 1.3 min. Analytes were eluted using a Waters Acquity UPLC pump with a well-plate autosampler maintained at 8 ^{o}C. The flow rate was maintained at 0.45 mL/min, and the column temperature was 55 ^{o}C.

Mass spectrometry analysis was performed using the Synapt G2-S QToF-MS with an ESI source in a negative or positive ion mode. MS operating conditions were as follows: cone voltage, 20 V; capillary voltage, 1.8 kV; source temperature, 110 ˚C; desolvation temperature, 350 ˚C; cone gas flow rate, 10 L/h; and desolvation gas flow, 1,000 L/h. The analyzer was operated with an extended dynamic range at 10,000 resolution (fwhm at *m/z* 554) with an acquisition time of 0.1s. The Synapt G2-S ToF MSE mode was used to collect data with the T-wave element alternated between low (MS) and high (MSE) energy states in which the transfer T-wave element voltage ranged from 10–25 V. Leucine enkephalin (400 pg/μL) was infused at a rate of 10 μL/min for mass correction. MassLynx V4.1 software (Waters) was used for instrument control, acquisition, and mass analysis. The structural information of the degradation products was obtained by the state-of-the-art MSE function that allows the simultaneous acquisition of both MS and MS/MS fragmentation during a single chromatographic run.[1, 2]

Quantification of all target PFAAs was made using extracted ion currents (10 ppm mass window). It was based on their *m/z* values and UPLC retention times relative to six-point external calibration standard curves.

HRPIS experiments

The identification of thermal decomposition products of PFAS was conducted in two major steps.[2] In brief, high-resolution precursor ion scans were performed after aligning MS and MS/MS extracted ion chromatograms generated from UPLC–ESI-ToF–MSE data using the MassLynx V4.1 software. The parent MS and characteristic MS/MS spectra aligned with characteristic fragment ions were then examined and candidate PFAS parent compounds were identified by HRPIS[2] with a mass error tolerance of 10 ppm.

Determination of extraction efficiency

We previously compared the different approaches for extracting PFAS from spent GAC.[3] In these experiments, GAC particles (0.07 g) in pre-cleaned polypropylene vials were spiked with a known volume of 1 × 10^{-3} mol/L PFAS stock solution in methanol. Then 10-mL methanol amended with 100 mmol/L NH_4Ac was added to the tubes to extract PFAS from GAC. The liquid phase was sampled and microfiltered (0.45 μm nylon filter; Thermo Scientific™ Target2™). The concentration of PFAS in the filtrate was determined and the mass was calculated to determine the recovery by comparing it with the spiked mass. The recovery rate varies from 79.2% to 111.8%[3]

for most of the PFAS investigated. Without the addition of NH_4Ac, the recovery is largely below 70%.

TD–Pyr–GC–MS method

The Frontier 3030D pyrolyzer, including an optional autosampler, is installed on top of the GC. This system allows for multiple-step heating, including TD at ≤ 300 °C (evolution of intact low MW compounds) and Pyr, typically at temperatures above 350 °C (evolution of thermal breakdown products of high MW species or thermally stable species). Following the different TD-Pyr steps, the gaseous products were concentrated in a cryogenic trapping system, introduced on the GC column, and analyzed by GC–MS. A Frontier 30-m Ultra Alloy capillary column (30 m; Frontier Labs Inc., Japan) was used with an inner diameter of 0.25 mm and a 5% diphenyldimethyl polysiloxane stationary phase with 0.25 μm film thickness. The MS analysis was performed with electron ionization in the mass range of 35-850 *m/z*. Ultra-pure helium (99.999%) was used as the carrier gas with a constant flow rate of 1.1 mL/min.

A known mass of PFAS chemical was placed in the Pyr furnace and heated at a rate of 400 °C /min from 50 °C to 200 °C to analyze thermal decomposition products generated at 200 °C. The temperature was maintained at 200 °C for 30 sec before sampling for GC–MS analysis. After sampling, the Pyr furnace temperature was increased from 200 °C to 300 °C at a rate of 400 °C /min and kept at 300 °C for 30 sec before sampling for GC–MS analysis of gaseous products generated at 300 °C. To analyze Analyses at different temperatures were performed on each of the PFAS samples (see below).

Two blank samples were prepared with clean, empty cups and analyzed before PFAS samples. If the baseline of the second blank was not clean, a third blank was prepared and analyzed. No perfluorinated species were found in blank samples.

We were able to analyze HFPO-DA, PFBA, and PFPeA by TD–Pyr–GC–MS. Not that the analysis of *one* PFAS sample using TD–Pyr–GC–MS by a commercial laboratory can cost $3,000–$5,000.

DFT calculations

A supercomputer (Intel Platinum 48 Core, Beijing Super Cloud Computing Center) was used to perform high-throughput DFT calculations of BDEs, also known as bond enthalpy, in PFECAs, short-chain PFCAs, and the unsaturated PFCA (i.e., PFMeUPA). A state-of-the-art M06-2X method[4] at a 3-zeta basis set of Def2-TZVP was employed using the state-of-the-art Gaussian 16 program.[5] The M06-2X method was chosen for the structural optimization, frequency analysis, and single-point energy calculation with 3-zeta basis set of Def2-TZVP at 298.15K in the gas phase.[4] Gaussian's input and output files were edited and viewed by GaussView 6. The Gibbs free energy, $G(T)$, and bond dissociation enthalpies (BDE) were calculated by Eq (S1) and (S2):

$$G(T) = (EE + GFE) \times 627.5094 \quad \text{(S1)}$$

$$BDE = G(T)_{\text{product}} - G(T)_{\text{reactant}} \quad \text{(S2)}$$

where EE represents the electronic energy of PFAS (Hartree, an unit of energy in the Hartree atomic units system); GFE, the thermal correction to $G(T)$ (Hartree); $G(T)_{\text{product}}$, represents the total Gibbs free energy of all products in each reaction (kcal/mol); and $G(T)_{\text{reactant}}$, the total Gibbs free energy of the reactant in each reaction (kcal/mol). BDEs for all bonds in HFPO-DA, HFPO-TA, HFPO-TeA, PFBA, PFPeA, PFMPA, and PFMeUPA were calculated. Based on experimental

data on intermediates (e.g., PFPrA from HFPO-DA), the reaction with the lowest BDE value was regarded as the most favorable thermal degradation pathway.

Possible PFBA thermal decomposition pathways

$$\mathrm{PFBA}\xrightarrow{\Delta}\begin{cases} \underset{random\ scission}{\mathrm{CF3-CF2^{\cdot}+{\cdot}CF2-COOH}\left(65.4\frac{\mathrm{Kcal}}{\mathrm{mol}}\right)\xrightarrow{+{\cdot}\mathrm{F}}\mathrm{CF3-COOH\ (TFA)}} \\ \mathrm{CF3^{\cdot}+{\cdot}CF2-CF2-COOH}\left(75.4\frac{\mathrm{Kcal}}{\mathrm{mol}}\right)\xrightarrow{+{\cdot}\mathrm{F}}\mathrm{CF3-CF2-COOH\ (PFPrA)} \\ \underset{end-chain\ scission/decarboxylation}{\mathrm{CF3-CF2-CF2^{\cdot}+{\cdot}COOH}\left(72.0\frac{\mathrm{Kcal}}{\mathrm{mol}}\right)\begin{cases}\xrightarrow{-{\cdot}\mathrm{F}}\mathrm{CF3-CF2=CF2\ (perfluoropropene)} \\ \xrightarrow{-\mathrm{CF2}}\mathrm{CF3-CF2^{\cdot}}\xrightarrow{+{\cdot}\mathrm{COOH}}\mathrm{CF3-CF2-COOH\ (PFPrA)}\end{cases}} \end{cases} \tag{S3}$$

Table S1. PFAS chemicals used in this study.

PFECAs (perfluoroalkyl ether carboxylic acids)	Acronyms	Purity	CAS #	Structure	SMILES
Perfluoro-2-methyl-3-oxahexanoic acid	HFPO-DA	97%	13252-13-6	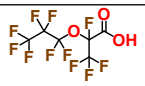	OC(=O)C(F)(OC(F)(F)C(F)(F)C(F)(F)F)C(F)(F)F
Perfluoro-2,5-dimethyl-3,6-dioxanonanoic acid	HFPO-TA	97%	13252-14-7	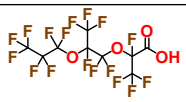	OC(=O)C(F)(OC(F)(F)C(F)(OC(F)(F)C(F)(F)C(F)(F)F)C(F)(F)F)C(F)(F)F
Pefluoro-2,5,8-trimethyl-3,6,9-trioxadecanoic acid	HFPO-TeA	95%	65294-16-8	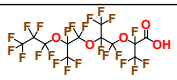	OC(=O)C(F)(OC(F)(F)C(F)(OC(F)(F)C(F)(OC(F)(F)C(F)(F)C(F)(F)F)C(F)(F)F)C(F)(F)F)C(F)(F)F
Perfluoro-3-methoxypropanoic acid	PFMPA	95%	377-73-1	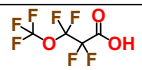	OC(=O)C(F)(F)C(F)(F)OC(F)(F)F
Perfluoro-3,6-dioxaheptanoic acid	PFO2HpA	98%	151772-58-6	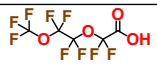	OC(=O)C(F)(F)OC(F)(F)C(F)(F)OC(F)(F)F
PFCAs	**Acronyms**	**Purity**	**CAS #**	**Structure**	
Perfluorobutyric acid (C4)	PFBA	≥99.5	375-22-4	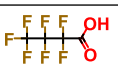 (C4)	OC(=O)C(F)(F)C(F)(F)C(F)(F)F
perfluoropentanoic acid (C5)	PFPeA	97%	2706-90-3		
Perfluoroheptanoic acid (C6)	PFHpA	≥97%	375-85-9		
Perfluorooctanoic acid (C8)	PFOA	95%	335-67-1		
Perfluorononanoic acid (C9)	PFNA	97%	375-95-1		
Perfluorodecanoic acid (C10)	PFDA	98%	335-76-2		
Perfluoroundecanoic acid (C11)	PFUnDA	95%	2058-94-8		
Unsaturated PFCA	**Acronyms**	**Purity**	**CAS #**	**Structure**	**SMILES**
4-(trifluoromethyl)hexafluoropent-2-enoic acid	PFMeUPA	97%	103229-89-6	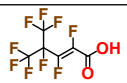	C(=C(/C(C(F)(F)F)(C(F)(F)F)F)\F)(\C(=O)O)/F
PFSAs	**Acronyms**	**Purity**	**CAS #**	**Structure**	**SMILES**
Perfluorobutanesulfonic acid potassium salt (C4)	PFBS	98.0%	29420-49-3	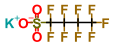 (C4)	C(C(C(F)(F)S(=O)(=O)[O-])(F)F)(C(F)(F)F)(F)F.[K+]
Perfluorohexanesulfonic acid potassium salt (C6)	PFHxS	≥98.0 %	3871-99-6		
Perfluorooctanesulfonic acid potassium salt (C8)	PFOS	≥98.0 %	2795-39-3		

All PFAS chemicals were purchased from Sigma–Aldrich.

Table S2. BDEs of HFPO-DA.

PFAS	Sequence	G(*T*)	BDE (Kcal/mol)
HFPO-DA	CF_3-CF_2-CF_2-O-CF(CF_3)-COOH	-1553.312539	
	CF_3-CF_2-CF_2·	-813.233055	79.6
	·O-CF(CF_3)-COOH	-739.952607	
	CF_3-CF_2-CF_2-O·	-888.451761	74.2
	·CF(CF_3)-COOH	-664.74252	
	CF_3-CF_2-CF_2-O-CF(CF_3)·	-1364.093419	71.2
	·COOH	-189.105688	
	CF_3·	-337.614015	77.1
	·CF2-CF2-O-CF(CF3)-COOH	-1215.575725	
	CF_3-CF_2·	-575.426334	76.1
	·CF_2-O-CF(CF_3)-COOH	-977.764859	
	CF_3-CF_2-CF_2-O-CF(·)-COOH	-1215.58953	69.6
	CF_3·	-337.612099	
	CF_3-CF_2-CF_2-O-CF(CF_3)-CO·	-1477.41267	100.1
	·OH	-75.74036	
	·F	-99.748541	
	·CF_2-CF_2-CF_2-O-CF(CF_3)-COOH	-1453.382954	113.6
	CF_3-CF(·)-CF_2-O-CF(CF_3)-COOH	-1453.393842	106.8
	CF_3-CF_2-CF(·)-O-CF(CF_3)-COOH	-1453.390428	108.9
	CF_3-CF_2-CF_2-O-C(·)(CF_3)-COOH	-1453.409519	96.9
	CF_3-CF_2-CF_2-O-CF(CF_2(·))-COOH	-1453.380619	115.1
	CF_3-CF_2-CF_2-O-CF(CF_3)-COO·	-1552.632638	107.4
	·H	-0.508793	
	PFBA:CF_3-CF_2-CF_2-COOH	-1002.453442	-72.0
	CF_2	-237.740076	41.8
	CF_3-CF_2·	-575.426332	
	PFPrA:CF_3-CF_2-COOH	-764.650124	-74.1
	CF_3-CF_2-OH	-651.327167	-100.7
	CF_3-CF_2-O·	-650.646133	108.1
	CF_3-COF	-550.8659	1.3
	CF_3-CF_2-CO·	-688.747647	101.7
	CF_3-CH_2-CO·	-490.243044	15.8
	CH_2	-39.123645	1.3
	CF_3-CH_2-COOH	-566.140985	18.6
	TFA:CF_3-COOH	-526.842746	109.6
	CF_3-CF_2-CF_2-O-CF=CF_2	-1264.243824	63.4

Table S3. BDEs of HFPO-TA.

PFAS	Sequence	G(*T*)	BDE (Kcal/mol)
HFPO-TA	CF_3-CF_2-CF_2-O-CF(CF_3)-CF_2-O-CF(CF_3)-COOH	-2341.964749	
	CF_3-CF_2-CF_2·	-813.233055	78.5
	·O-CF(CF_3)-CF_2-O-CF(CF_3)-COOH	-1528.606552	
	CF_3-CF_2-CF_2-O·	-888.451761	77.9
	·CF(CF_3)-CF_2-O-CF(CF_3)-COOH	-1453.388777	
	CF_3-CF_2-CF_2-O-CF(CF_3)-CF_2·	-1601.890257	75.4
	·O-CF(CF_3)-COOH	-739.954354	
	CF_3-CF_2-CF_2-O-CF(CF_3)-CF_2-O·	-1677.10784	75.4
	·CF(CF_3)-COOH	-664.736712	
	CF_3-CF_2-CF_2-O-CF(CF_3)-CF_2-O-CF(CF_3)·	-2152.750138	68.4
	·COOH	-189.105688	
	CF_3·	-337.614015	76.9
	·CF_2-CF_2-O-CF(CF_3)-CF_2-O-CF(CF_3)-COOH	-2004.228208	
	CF_3-CF_2·	-575.426334	76.0
	·CF_2-O-CF(CF_3)-CF_2-O-CF(CF_3)-COOH	-1766.417313	
	CF_3-CF_2-CF_2-O-CF(CF_3)·	-1364.088423	73.2
	·CF_2-O-CF(CF_3)-COOH	-977.759719	
	CF_3-CF_2-CF_2-O-CF(·)-CF_2-O-CF(CF_3)-COOH	-2004.237566	71.0
	CF_3-CF_2-CF_2-O-CF(CF_3)-CF_2-O-CF(·)-COOH	-2004.241153	68.8
	CF_3-CF_2-CF_2-O-CF(CF_3)-CF_2-O-CF(CF_3)-CO·	-2266.069485	97.2
	·OH	-75.74036	
	·F	-99.748541	
	·CF_2-CF_2-CF_2-O-CF(CF_3))-CF_2-O-CF(CF_3)-COOH	-2242.034955	113.7
	CF_3-CF(·)-CF_2-O-CF(CF_3))-CF_2-O-CF(CF_3)-COOH	-2242.044995	107.4
	CF_3-CF_2-CF(·)-O-CF(CF_3))-CF_2-O-CF(CF_3)-COOH	-2242.045754	107.0
	CF_3-CF_2-CF_2-O-C(·)(CF_3))-CF_2-O-CF(CF_3)-COOH	-2242.054898	101.2
	CF_3-CF_2-CF_2-O-CF(CF_2(·))-CF_2-O-CF(CF_3)-COOH	-2242.037578	112.1
	CF_3-CF_2-CF_2-O-CF(CF_3)-CF(·)-O-CF(CF_3)-COOH	-2242.043057	108.7
	CF_3-CF_2-CF_2-O-CF(CF_3)-CF2-O-C(·)(CF_3))-COOH	-2242.060282	97.8
	CF_3-CF_2-CF_2-O-CF(CF_3)-CF_2-O-CF(CF_2(·))-COOH	-2242.033061	114.9
	CF_3-CF_2-CF_2-O-CF(CF_3))-CF_2-O-CF(CF_3)-COO·	-2341.289742	104.3
	·H	-0.508793	

Table S4. BDEs of HFPO-TeA.

PFAS	Sequence	G(*T*)	BDE (Kcal/mol)
HFPO-TeA	CF_3-CF_2-CF_2-O-CF(CF_3)-CF_2-O-CF(CF_3)-CF_2-O-CF(CF_3)-COOH	-3130.620629	77.1
	CF_3-CF_2-CF_2·	-813.233055	
	·O-CF(CF_3)-CF_2-O-CF(CF_3)-CF_2-O-CF(CF_3)-COOH	-2317.264657	
	CF_3-CF_2-CF_2-O·	-888.451761	77.5
	·CF(CF_3)-CF_2-O-CF(CF_3)-CF_2-O-CF(CF_3)-COOH	-2242.045307	
	CF_3-CF_2-CF_2-O-CF(CF_3)-CF_2·	-1601.890257	77.7
	·O-CF(CF_3)-CF_2-O-CF(CF_3)-COOH	-1528.606559	
	CF_3-CF_2-CF_2-O-CF(CF_3)-CF_2-O·	-1677.10784	77.8
	·CF(CF_3)-CF_2-O-CF(CF_3)-COOH	-1453.388766	
	CF_3-CF_2-CF_2-O-CF(CF_3)-CF_2-O-CF(CF_3)-CF_2·	-2390.546803	75.0
	·O-CF(CF_3)-COOH	-739.954354	
	CF_3-CF_2-CF_2-O-CF(CF_3)-CF_2-O-CF(CF_3)-CF_2-O·	-2465.764497	74.9
	·CF(CF_3)-COOH	-664.736712	
	CF_3-CF_2-CF_2-O-CF(CF_3)-CF_2-O-CF(CF_3)-CF_2-O-CF(CF_3)·	-2941.406309	68.2
	·COOH	-189.105688	
	CF_3·	-337.614015	76.8
	·CF_2-CF_2-O-CF(CF_3)-CF_2-O-CF(CF_3)-CF_2-O-CF(CF_3)-COOH	-2792.88427	
	CF_3-CF_2·	-575.426334	74.7
	·CF_2-O-CF(CF_3)-CF_2-O-CF(CF_3)-CF_2-O-CF(CF_3)-COOH	-2555.075269	
	CF_3-CF_2-CF_2-O-CF(CF_3)·	-1364.088424	70.7
	·CF_2-O-CF(CF_3)-CF_2-O-CF(CF_3)-COOH	-1766.419561	
	CF_3-CF_2-CF_2-O-CF(·)-CF_2-O-CF(CF_3)-CF_2-O-CF(CF_3)-COOH	-2792.895628	69.6
	CF_3-CF_2-CF_2-O-CF(CF_3)-CF_2-O-CF(CF_3)·	-2152.746618	
	·CF_2-O-CF(CF_3)-COOH	-977.759727	71.7
	CF_3-CF_2-CF_2-O-CF(CF_3)-CF_2-O-CF(·)-CF_2-O-CF(CF_3)-COOH	-2792.894759	70.2
	CF_3-CF_2-CF_2-O-CF(CF_3)-CF_2-O-CF(CF_3)-CF_2-O-CF(·)-COOH	-2792.89898	67.5
	CF_3-CF_2-CF_2-O-CF(CF_3)-CF_2-O-CF(CF_3)-CF_2-O-CF(CF_3)-CO·	-3054.725719	97.0
	·OH	-75.74036	
	·F	-99.748541	
	·CF_2-CF_2-CF_2-O-CF(CF_3))-CF_2-O-CF(CF_3)-CF_2-O-CF(CF_3)-COOH	-3030.691078	113.6

	CF_3-CF(·)-CF_2-O-CF(CF_3))-CF_2-O-CF(CF_3)-CF_2-O-CF(CF_3)-COOH	-3030.70118	107.2
	CF_3-CF_2-CF(·)-O-CF(CF_3))-CF_2-O-CF(CF_3)-CF_2-O-CF(CF_3)-COOH	-3030.703336	105.9
	CF_3-CF_2-CF_2-O-C(·)(CF_3))-CF_2-O-CF(CF_3)-CF_2-O-CF(CF_3)-COOH	-3030.713093	99.8
	CF_3-CF_2-CF_2-O-CF(CF_2(·))-CF_2-O-CF(CF_3)-CF_2-O-CF(CF_3)-COOH	-3030.695099	111.1
	CF_3-CF_2-CF_2-O-CF(CF_3)-CF(·)-O-CF(CF_3)-CF_2-O-CF(CF_3)-COOH	-3030.702729	106.3
	CF_3-CF_2-CF_2-O-CF(CF_3)-CF_2-O-C(·)(CF_3)-CF_2-O-CF(CF_3)-COOH	-3030.711961	100.5
	CF_3-CF_2-CF_2-O-CF(CF_3)-CF_2-O-CF(CF_2(·))-CF_2-O-CF(CF_3)-COOH	-3030.695904	110.6
	CF_3-CF_2-CF_2-O-CF(CF_3)-CF_2-O-CF(CF_3)-CF(·)-O-CF(CF_3)-COOH	-3030.694184	111.6
	CF_3-CF_2-CF_2-O-CF(CF_3)-CF_2-O-CF(CF_3)-CF_2-O-C(·)(CF_3)-COOH	-3030.716696	97.5
	CF_3-CF_2-CF_2-O-CF(CF_3)-CF_2-O-CF(CF_3)-CF_2-O-CF(CF_2(·))-COOH	-3030.689959	114.3
	CF_3-CF_2-CF_2-O-CF(CF_3))-CF_2-O-CF(CF_3)-CF_2-O-CF(CF_3)-COO·	-3129.945458	104.4
	·H	-0.508793	

Table S5. BDEs of PFMeUPA.

PFAS	Sequence	G(*T*)	BDE (Kcal/mol)
PFMeUPA	F_3C-$CF(CF_3)$-CF=CF-COOH	-1278.332983	
	F_3C·	-337.614015	58.8
	F_3C-CF(·)-CF=CF-COOH	-940.625237	
	F_3C-C(F)(CF_3)·	-813.24455	81.5
	·CF=CF-COOH	-464.958501	
	F_3C-$CF(CF_3)$-CF	-951.134437	124.6
	CF-COOH	-326.999959	
	F_3C-$CF(CF_3)$-CF=CF·	-1089.086052	88.6
	·COOH	-189.105688	
	F_3C-$CF(CF_3)$-CF=CF-CO·	-1202.435888	98.4
	·OH	-75.74036	
	·F	-99.748541	
	F_2C(·)-$CF(CF_3)$-CF=CF-COOH	-1178.404586	112.9
	F_3C-C(CF_3)(·)-CF=CF-COOH	-1178.450607	84.0
	F_3C-$CF(CF_3)$-C(·)=CF-COOH	-1178.416649	105.3
	F_3C-$CF(CF_3)$-CF=C(·)-COOH	-1178.414004	107.0
	F_3C-$CF(CF_3)$-CF=CF-COO·	-1277.655641	105.8
	·H	-0.508793	

Table S6. BDEs of PFMPA.

PFAS	Sequence	G(*T*)	BDE (Kcal/mol)
PFMPA	F_3C-O-CF_2-CF_2-COOH	-1077.697526	
	F_3C·	-337.614015	91.8
	·O-CF_2-CF_2-COOH	-739.937232	
	F_3C-O·	-412.837209	89.2
	·CF_2-CF_2-COOH	-664.718096	
	F_3C-O-C(F_2)·	-650.663558	69.7
	·CF_2-COOH	-426.92295	
	F_3C-O-CF_2-C(F_2)·	-888.473636	74.2
	·COOH	-189.105688	
	F_3C-O-CF_2-CF_2-CO·	-1001.798102	99.8
	·OH	-75.74036	
	·F	-99.748541	
	F_2C(·)-O-CF_2-CF_2-COOH	-977.76497	115.5
	F_3C-O-CF(·)-CF_2-COOH	-977.77539	108.9
	F_3C-O-CF_2-CF(·)-COOH	-977.790429	99.5
	F_3C-O-CF_2-CF_2-COO(·)	-1077.018232	107.0
	·H	-0.508793	

Table S7. BDEs of PFBA.

PFAS	Sequence	G(*T*)	BDE (Kcal/mol)
PFBA	PFBA:CF3-CF2-CF2-COOH	-1002.453442	
	CF3-CF2-CF2·	-813.233055	72.0
	·COOH	-189.105688	
	CF3·	-337.614015	75.4
	·CF2-CF2-COOH	-664.719353	
	CF3-CF2·	-575.426334	65.4
	·CF2-COOH	-426.922951	
	·F	-99.748541	
	·CF2-CF2-CF2-COOH	-902.523309	114.0
	CF3-CF(·)-CF2-COOH	-902.53657	105.6
	CF3-CF2-CF(·)-COOH	-902.549616	97.4
	·H	-0.508793	106.9
	CF3-CF2-CF2-COO·	-1001.774246	
	CF3-CF2-CF2-CO·	-926.554975	99.2
	·OH	-75.74036	

Table S8. BDEs of PFPeA.

PFAS	Sequence	G(*T*)	BDE (Kcal/mol)
PFPeA	CF_3-CF_2-CF_2-CF_2-COOH	-1240.258555	
	CF_3-CF_2-CF_2-CF_2·	-1051.037884	72.2
	·COOH	-189.105688	
	CF_3·	-337.614015	75.0
	·CF_2-CF_2-CF_2-COOH	-902.525015	
	CF_3-CF_2·	-575.426334	70.8
	·CF_2-CF_2-COOH	-664.719353	
	CF_3-CF_2-CF_2·	-813.233475	64.1
	·CF_2-COOH	-426.922951	
	CF_3-CF_2-CF_2-CF_2-CO·	-1164.359065	99.9
	·OH	-75.74036	
	·F	-99.748541	113.5
	CF_2(·)-CF_2-CF_2-CF_2-COOH	-1140.329073	
	CF_3-CF(·)-CF_2-CF_2-COOH	-1140.342679	105.0
	CF_3-CF_2-CF(·)-CF_2-COOH	-1140.343539	104.5
	CF_3-CF_2-CF_2-CF(·)-COOH	-1140.354964	97.3
	CF_3-CF_2-CF_2-CF_2--COO·	-1239.579189	107.0
	·H	-0.508793	
	CF_3-CF_2-CF=CF_2	-951.209463	50.1
	CF_2	-237.740076	40.6
	CF_3-CF_2-CF_2·	-813.233055	
	PFBA: CF_3-CF_2-CF_2-COOH	-1002.453442	-72.0
	CF_3-CF=CF_2	-713.402379	51.5

	CF_3-CF_2·	-575.426332	41.8
	PFPrA: CF_3-CF_2-COOH	-764.650124	-74.1
	CF_2=CF_2	-475.573578	65.4
	·CF_3	-337.614015	45.3
	TFA: CF_3-COOH	-526.842746	-77.2

Figures

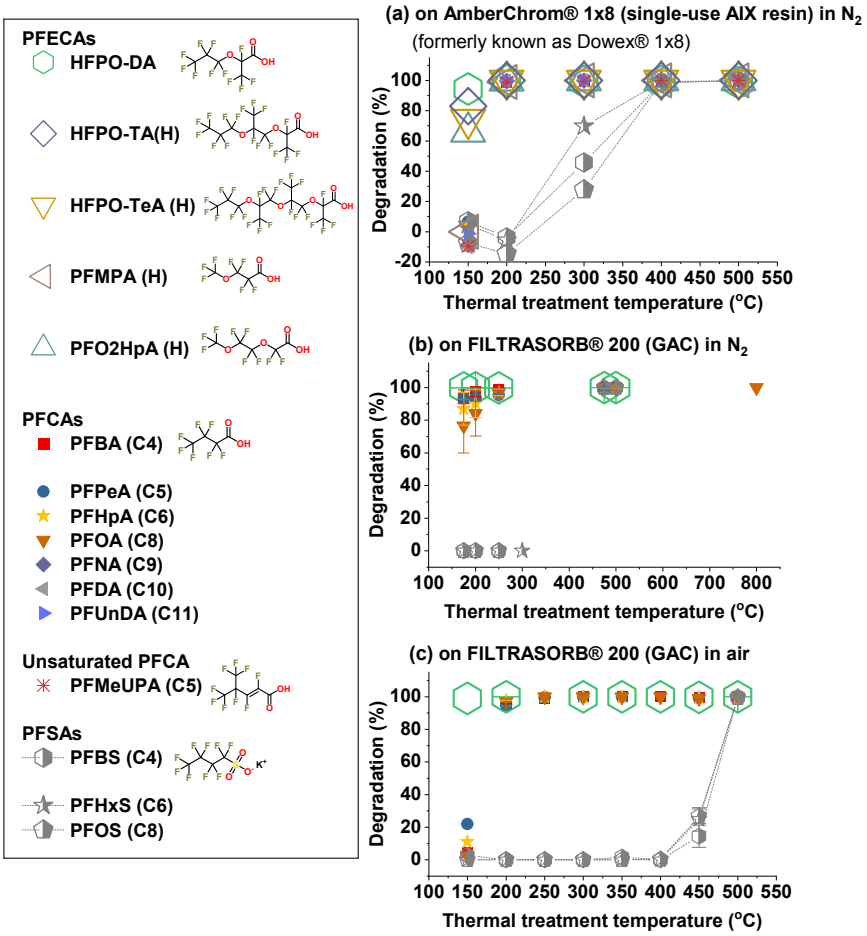

Figure S1. Thermal decomposition of a mixture of HPFO-DA, PFCAs, and PFSAs pre-adsorbed on (a) a single-use resin and (b, c) GAC.[3] Thermal treatment was conducted at different temperatures for 30 min. In selected experiments, a high (H) initial mass of a mixture of PFECAs (e.g., PFMPA (H)) was directly added to the resin to estimate the maximum percentage removal of PFCEAs upon heating.

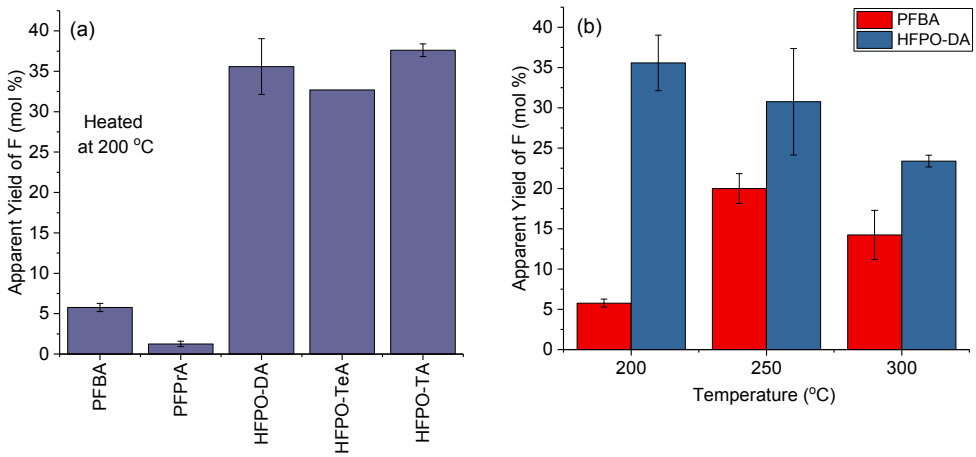

Figure S2. Apparent yield of F from PFCAs and PFECAs (initial mass: 1.2 μmol) heated for 30 min at different temperatures with the presence of GAC (0.1 g) to mimic the regeneration process (<300 °C) of PFAS-laden GAC.

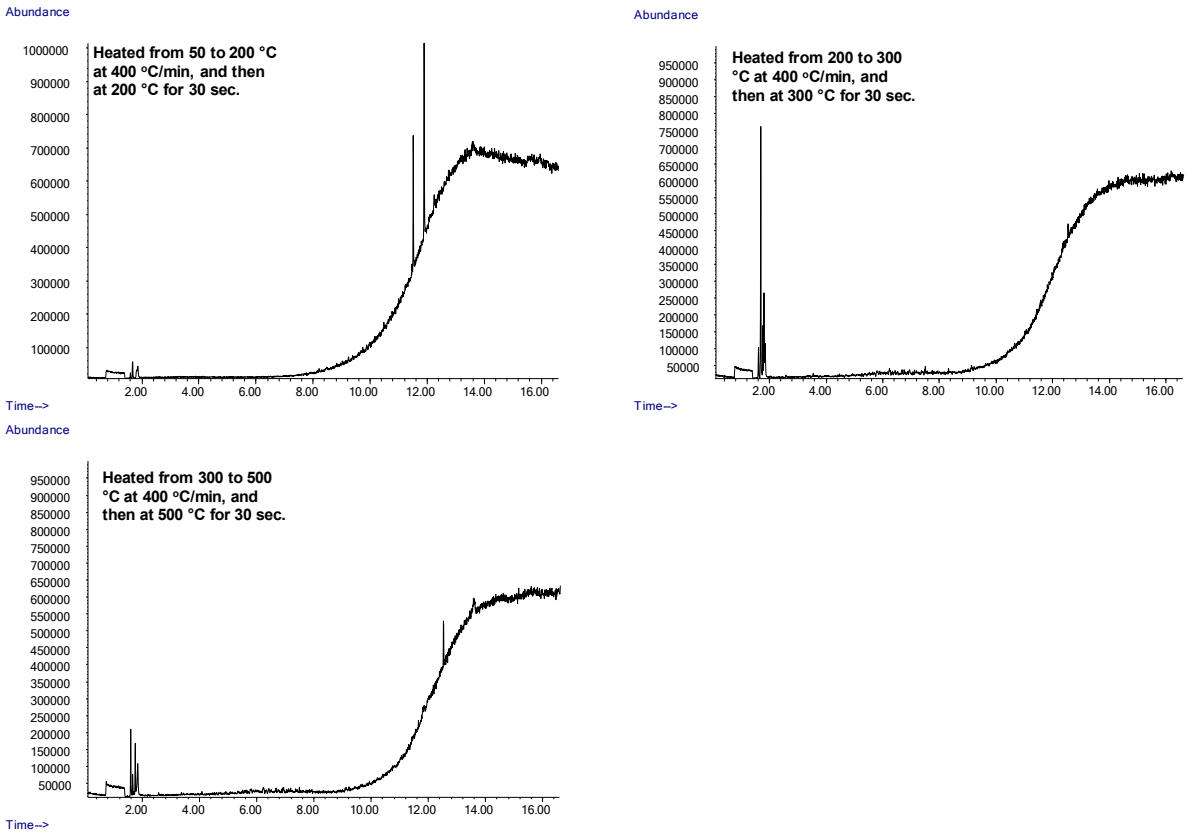

Figure S3. TD–Pyr–GC–MS chromatograms of HFPO-DA at 200–500 °C.

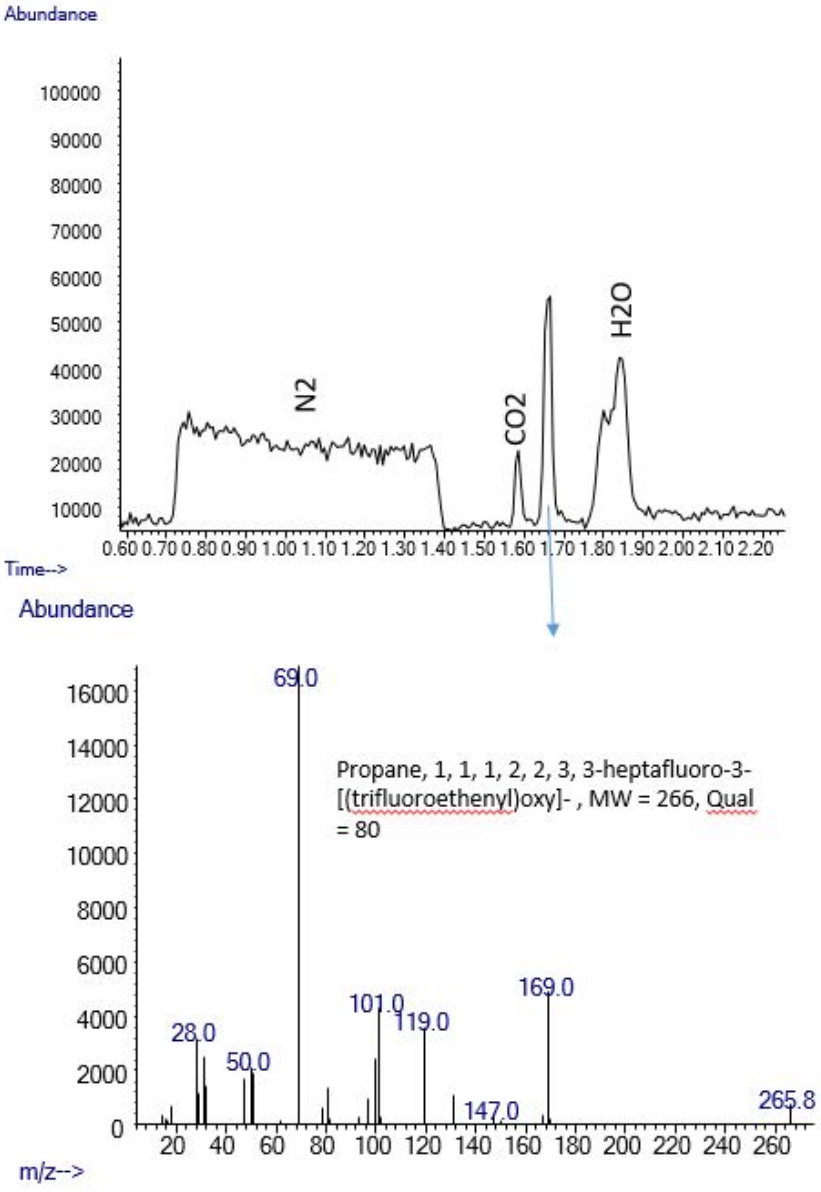

Figure S4. TD–Pyr–GC–MS chromatogram and spectrum of HFPO-DA at 200 °C.

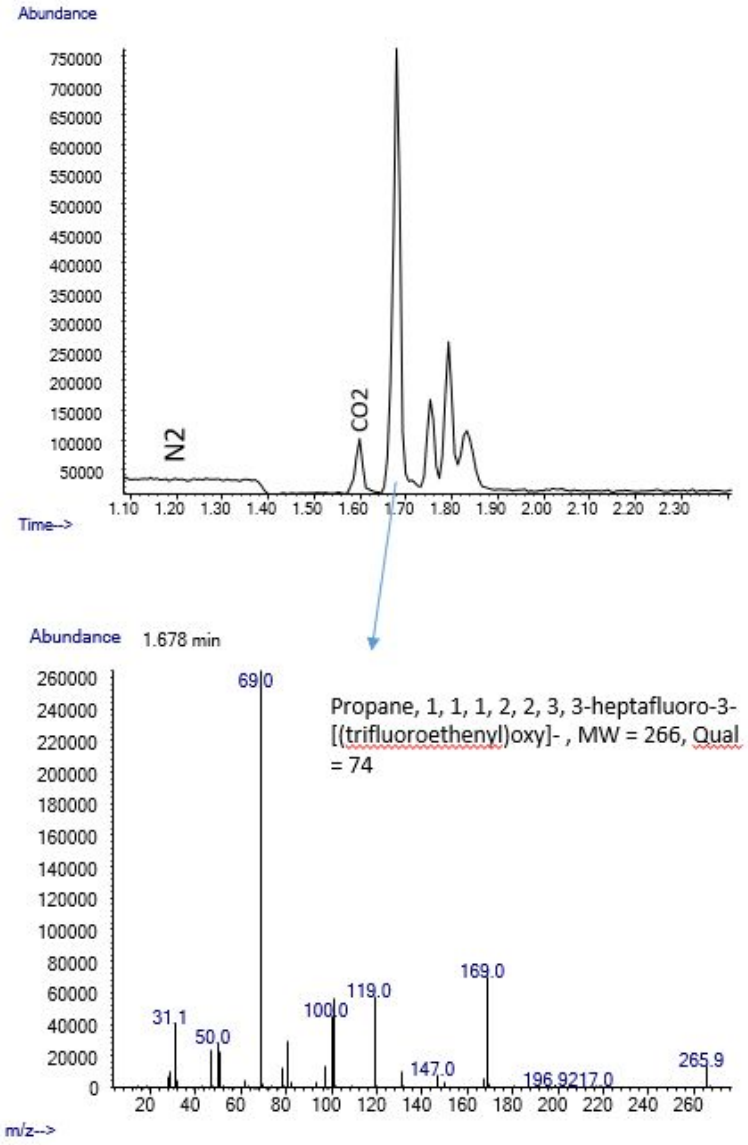

Figure S5. TD–Pyr–GC–MS chromatogram and spectrum of HFPO-DA at 300 °C.

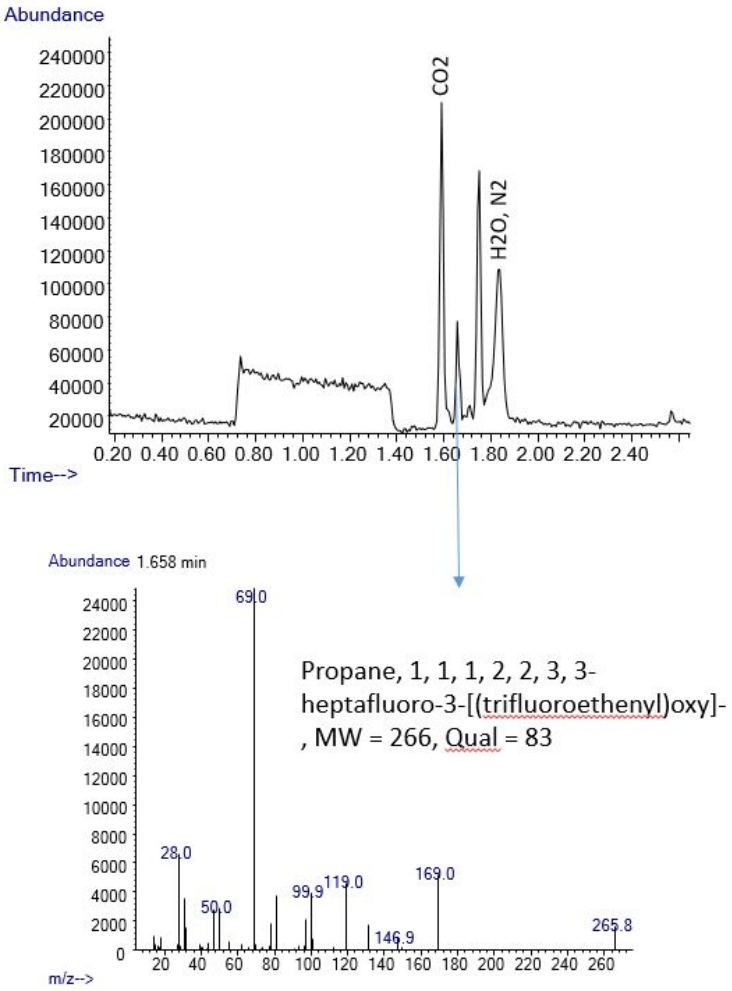

Figure S6. TD–Pyr–GC–MS chromatogram and spectrum of HFPO-DA at 500 °C.

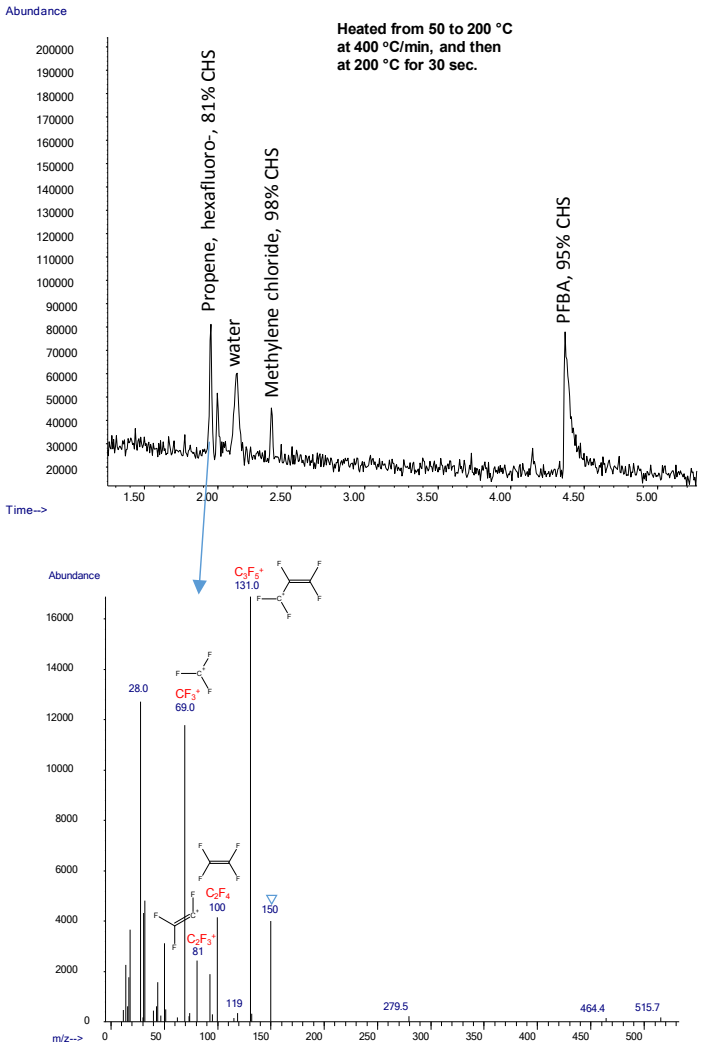

Figure S7. TD–Pyr–GC–MS chromatogram and spectrum of PFBA heated at 200 °C.

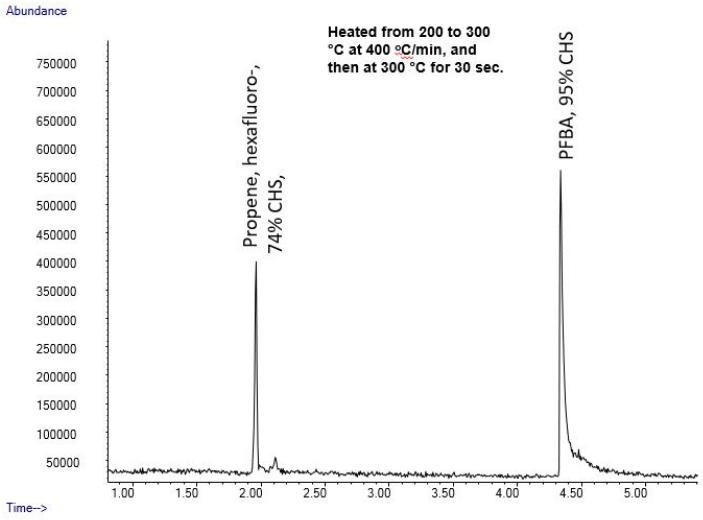

Figure S8. TD–Pyr–GC–MS chromatogram of PFBA heated at 300 °C.

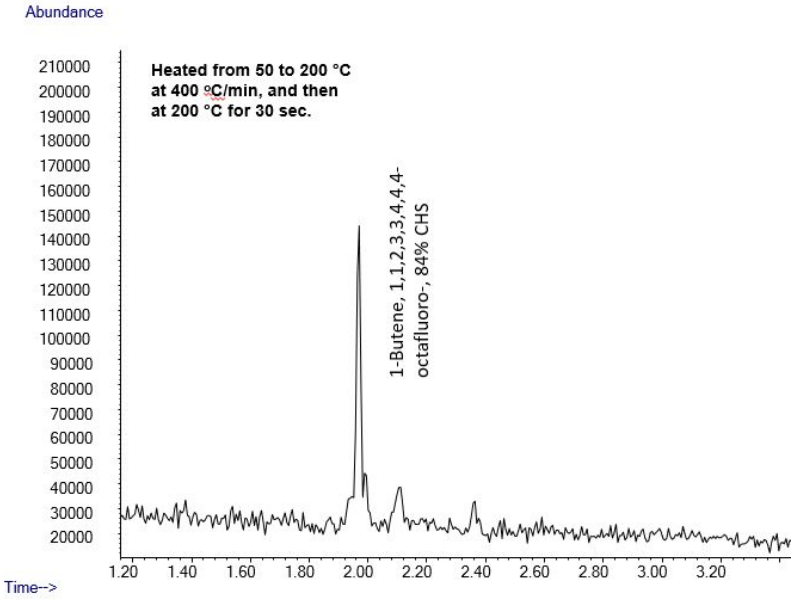

Figure S9. TD–Pyr–GC–MS chromatogram of PFPeA heated at 200 °C.

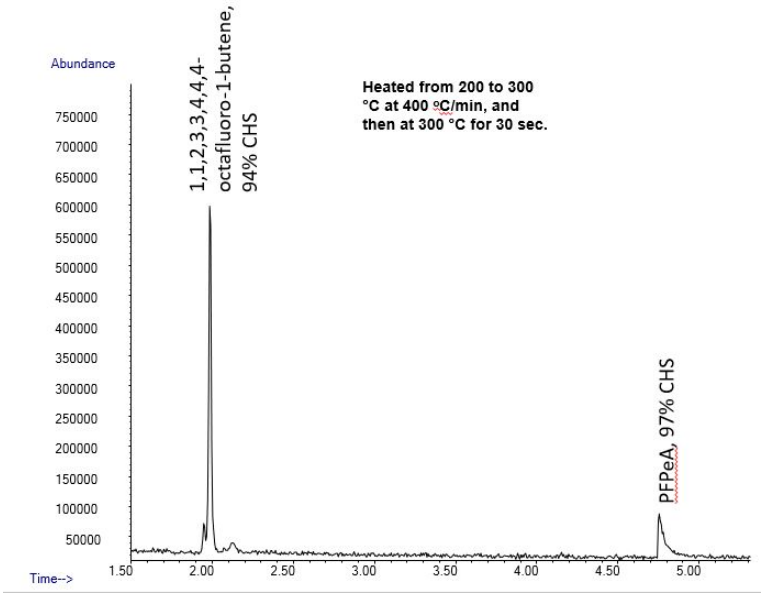

Figure S10. TD–Pyr–GC–MS chromatogram of PFPeA heated at 300 °C.

References cited in the Supporting Information:

1. Waters., An overview of the principles of MS^E, the engine that drives MS performance. In Waters Corporation: Milford, MA, 2011; pp 1-6.

2. Xiao, F.; Golovko, S. A.; Golovko, M. Y., Identification of novel non-ionic, cationic, zwitterionic, and anionic polyfluoroalkyl substances using UPLC-TOF-MS(E) high-resolution parent ion search. *Anal Chim Acta* **2017,** *988*, 41-49. doi:10.1016/j.aca.2017.08.016

3. Xiao, F.; Sasi, P. C.; Yao, B.; Kubatova, A.; Golovko, S. A.; Golovko, M. Y.; Soli, D., Thermal stability and decomposition of perfluoroalkyl substances on spent granular activated carbon. *Environ Sci Tech Let* **2020,** *7*(5), 343-350. doi:10.1021/acs.estlett.0c00114

4. Zhao, Y.; Truhlar, D. G., The M06 suite of density functionals for main group thermochemistry, thermochemical kinetics, noncovalent interactions, excited states, and transition elements: two new functionals and systematic testing of four M06-class functionals and 12 other functionals. *Theoretical Chemistry Accounts* **2008,** *120*(1), 215-241. doi:10.1007/s00214-007-0310-x

5. Frisch, M. J.; Trucks, G. W.; Schlegel, H. B.; Scuseria, G. E.; Robb, M. A.; Cheeseman, J. R.; Scalmani, G.; Barone, V.; Petersson, G. A.; Nakatsuji, H.; Li, X.; Caricato, M.; Marenich, A. V.; Bloino, J.; Janesko, B. G.; Gomperts, R.; Mennucci, B.; Hratchian, H. P.; Ortiz, J. V.; Izmaylov, A. F.; Sonnenberg, J. L.; Williams; Ding, F.; Lipparini, F.; Egidi, F.; Goings, J.; Peng, B.; Petrone, A.; Henderson, T.; Ranasinghe, D.; Zakrzewski, V. G.; Gao, J.; Rega, N.; Zheng, G.; Liang, W.; Hada, M.; Ehara, M.; Toyota, K.; Fukuda, R.; Hasegawa, J.; Ishida, M.; Nakajima, T.; Honda, Y.; Kitao, O.; Nakai, H.; Vreven, T.; Throssell, K.; Montgomery Jr., J. A.; Peralta, J. E.; Ogliaro, F.; Bearpark, M. J.; Heyd, J. J.; Brothers, E. N.; Kudin, K. N.; Staroverov, V. N.; Keith, T. A.; Kobayashi, R.; Normand, J.; Raghavachari, K.; Rendell, A. P.; Burant, J. C.; Iyengar, S. S.; Tomasi, J.; Cossi, M.; Millam, J. M.; Klene, M.; Adamo, C.; Cammi, R.; Ochterski, J. W.; Martin, R. L.; Morokuma, K.; Farkas, O.; Foresman, J. B.; Fox, D. J. *Gaussian 16 Rev. A.03*, Wallingford, CT, 2016.